Identification of novel *Trypanosoma cruzi* proteasome inhibitors using a luminescence-based high-throughput screening assay.

Filip Zmuda[†], *Lalitha Sastry*[†], *Sharon M. Shepherd*[‡], *Deuan Jones*[†], *Alison Scott*[‡], *Peter D. Craggs*[⊥], *Alvaro Cortes*[⊥], *David W. Gray**[†], *Leah S. Torrie*[†], *Manu De Rycker**[†]

[†]Drug Discovery Unit, Wellcome Centre for Anti-Infectives Research, School of Life Sciences, University of Dundee, Dow Street, Dundee DD1 5EH, United Kingdom.

[‡]Protein Production Team, Wellcome Centre for Anti-Infectives Research, School of Life Sciences, University of Dundee, Dow Street, Dundee DD1 5EH, United Kingdom.

[⊥]Screening Compound Profiling and Mechanistic Biology, Platform Technology and Science, GlasoSmithKline, Gunnelswood Road, Stevenage SG1 2NY, United Kingdom.

Corresponding Author Information:

* E-mail: d.w.gray@dundee.ac.uk. Phone: +44 (0) 1382 386247

* E-mail: m.derycker@dundee.ac.uk. Phone: +44 (0) 1382 386211

Abstract

Chagas' disease, caused by the protozoan parasite *Trypanosoma cruzi*, is a potentially life-threatening condition that has become a global issue. Current treatment is limited to two medicines that require prolonged dosing and are associated with multiple side effects, which often lead to treatment discontinuation and failure. One way to address these shortcomings is through target-based drug discovery on validated *T. cruzi* protein targets. One such target is the proteasome, which plays a crucial role in protein degradation and turnover, through chymotrypsin-, trypsin-, and caspase-like catalytic activities. In order to initiate a proteasome drug discovery programme, we isolated

proteasomes from *T. cruzi* epimastigotes and characterized their activity using a commercially available glow-like luminescence-based assay. We developed a high-throughput biochemical assay for the chymotrypsin-like activity of the *T. cruzi* proteasome, which was found to be sensitive, specific, and robust, but prone to luminescence technology interference. To mitigate this, we have also developed a counter-screen assay that identifies potential interferers at the level of both the luciferase enzyme reporter and the mechanism responsible for a glow-like response. Interestingly, we also found that the peptide substrate for chymotrypsin-like proteasome activity was not specific, and was likely partially turned over by other catalytic sites of the protein. Finally, we utilised these biochemical tools to screen 18,098 compounds exploring diverse drug-like chemical space, which allowed us to identify 39 hits that were active in the primary screening assay ($pIC_{50} \geq 4$) and inactive in the counter-screen assay ($pIC_{50} < 4$).

Introduction

Chagas' disease is a parasitic disease caused by the kinetoplastid parasite *Trypanosoma cruzi*. The disease is not only a problem in the endemic regions of Latin America but also more globally because of migration (1,2). Disease progression is characterized by an initial acute phase with symptoms such as fever and local inflammation followed by a long symptom-less indeterminate phase. In a subset of people, the disease will develop into a symptomatic chronic phase with cardiomyopathy and mega-organ disease as the main manifestations. Approximately 2% of infected people will develop cardiac problems annually (3), with an associated death toll of around 10,000 per year (2). Treatment for Chagas' disease is currently limited to the two nitroheterocyclic drugs benznidazole and nifurtimox. Benznidazole is typically used as front-line treatment as it is better tolerated than nifurtimox, notwithstanding a 10% treatment discontinuation rate due to its own side effects (4). New, better tolerated, medicines are urgently required but their development has proven very difficult, as exemplified by the failure in clinical trials of the only two new candidate treatments; posaconazole and fos-ravuconazole (5,6). Many efforts are ongoing to identify new starting points for drug discovery, often through large scale phenotypic screening (7–12). Target-based screening, where a

particular protein is assayed in its purified state, is an alternative approach with the advantages of more straightforward understanding of chemistry structure-activity-relationships (SAR) due to the absence of any cell membranes, a direct relationship between compound affinity and target inhibition or binding, and the opportunity to generate structural information to guide chemistry design. Lack of translation of target inhibition to parasite death is an important risk when investing in such a programme, and selecting well-validated targets is essential. One powerful method to identify suitable protein targets is by determining the mode-of-action of compounds that show the desired phenotypic effects in terms of parasite killing. Recently, the proteasome was identified as a promising drug target for kinetoplastid diseases through mode-of-action determination of promising phenotypically active compounds (GNF6702 and GSK3494245/DDD01305143) (9,13). The proteasome is a key component of the ubiquitin-proteasome protein degradation system and plays an important role in many cellular processes, including protein turnover and cell signalling (14). In eukaryotes, the proteasome comprises of a central 20S cylindrical structure and two regulatory 19S complexes on either end of the 20S core. The 20S unit is made up of two outer (α) and two inner (β) polypeptide rings, where three of the β-type subunits are involved in chymotrypsin-, trypsin-, and caspase-like catalytic activities (15,16). The proteasome is a well-exploited target in drug discovery for a variety of indications, including cancer, inflammation and infectious diseases (17). In terms of parasitic diseases, the *Plasmodium* proteasome is well characterized and proof of concept that selective inhibition is possible has opened the route to development of new malaria drugs targeting the proteasome (18). GNF6702 is active against *Leishmania donovani*, *Trypanosoma brucei*, and *T. cruzi* both *in vitro* and *in vivo* whilst showing no toxicity against mammalian cells and GSK3494245/DDD01305143 is a pre-clinical candidate for visceral leishmaniasis developed from a *T. cruzi* screening hit, demonstrating that the proteasome is a suitable drug target across the kinetoplastid parasites. These compounds exert their effect on the parasites through the selective inhibition of the chymotrypsin-like activity of the parasite proteasome, and not the caspase- or trypsin-like activities (9,13).

Attrition in drug discovery programmes is high, and even compounds that demonstrate proof-of-concept efficacy in animal models frequently fail at later stages in the drug development process, often for target-unrelated reasons (19). Once a validated target has been identified, it is therefore sensible to generate multiple chemical classes of inhibitors. With this in mind, we have started a hit discovery programme for the *T. cruzi* proteasome chymotrypsin-like activity. Here we present the development of a luminescence-based high-throughput screening (HTS) assay using partially purified *T. cruzi* proteasomes, as well as a technology interference counter screen assay, which we then used to screen two diverse sets of compounds (18,098 compounds in total) in an effort to identify potential new starting points for a drug discovery programme against Chagas' disease.

Results and Discussion

T. cruzi proteasome characterization.

Proteasomes were harvested from cleared epimastigote lysates through ultracentrifugation, followed by partial purification using size-exclusion chromatography. In order to confirm the presence of enzymatic activity, chymotrypsin-, trypsin-, and caspase-like activities of the proteasome were measured using luminogenic versions of established peptide substrates (16,20) and a commercially available glow-response luminescence-based assay system (20). All three types of catalytic activities were found to be present in the pooled partially purified *T. cruzi* proteasome material. To further profile the isolated protein, the catalytic activities of the proteasome were measured over time in the presence of the irreversible proteasome inhibitor epoxomicin (21,22). The degree of inhibition of the chymotrypsin-like activity was the highest, followed by trypsin- and caspase-like activities (Figure 1), which is consistent with previous literature reports (22). The characteristic plateau of the kinetic curves in the absence of inhibitor compound corresponded to steady state conditions, where the rate of substrate consumption by the proteasome was equal to the rate of product consumption by the luciferase reporter enzyme (20). In the case of chymotrypsin-like activity, steady state conditions were

established within approximately 15 minutes and were maintained for the remainder of the 75 minute kinetic experiment.

High-throughput primary screening assay development.

Following the validation of the *T. cruzi* proteasome purification and isolation methodology, we diverted our efforts towards the optimization of the commercially available proteasome chymotrypsin-like activity luminescence-based assay for HTS. In the presence of a fixed amount of chymotrypsin-like substrate (i.e. suc-Leu-Leu-Val-Tyr-aminoluciferin) and under steady state conditions, the luminescence response was shown to be linearly proportional (R^2 = 0.9998) to the amount of *T. cruzi* proteasome up to a top concentration equivalent to a 1 in 2 dilution of the stock material (i.e. a concentration multiplication factor (CMF) = 0.5) (Figure 2 a). Steady state conditions were established rapidly for all of the tested concentrations of *T. cruzi* proteasome and were maintained throughout the course of the kinetic experiment with the exception of the top protein concentration (i.e. undiluted stock), where a drop-off in luminescence response was observed after approximately 30 minutes (Figure 2 b). This loss of steady state was likely a consequence of substrate depletion. By varying the concentration of suc-Leu-Leu-Val-Tyr-aminoluciferin in the presence of a fixed amount of *T. cruzi* proteasome, substrate inhibition was observed at a concentration of 600 µM during pre-steady state conditions (Figure 3 a). This is in line with the work of Stein *et al*, who also reported proteasome chymotrypsin-like activity inhibition at high concentrations of a fluorescence tagged variant of the suc-Leu-Leu-Val-Tyr peptide substrate (i.e. suc-Leu-Leu-Val-Tyr-AMC) (23). Utilising the Z factor as a measure of assay quality, where values ≥0.5 are generally accepted as sufficient for HTS (24), a 1 in 8 dilution (CMF = 0.125) of the stock *T. cruzi* proteasome preparation and a suc-Leu-Leu-Val-Tyr-aminoluciferin substrate concentration of 20 µM (final assay concentrations) were found to be optimal, affording Z factor values of >0.75 at steady state. Under these assay conditions, the apparent steady-state K_m for the suc-Leu-Leu-Val-Tyr-aminoluciferin substrate was found to be

93.5 µM (95% CI = 78.8–108.4 µM) (Figure 3 b), which was only marginally higher than the approximate value of 60 µM that was reported by O'Brien *et al* using a similar assay platform in a cellular system (20). Finally, as our screening compound libraries are formulated in dimethyl sulfoxide (DMSO), the tolerance of the biochemical assay to this solvent was investigated. We found that the maximum tested concentration of DMSO (1% v/v final assay concentration) was well tolerated by the system and had a negligible effect on the luminescence response (Figure S2).

High-throughput primary screening assay validation.

In order to validate the biochemical assay and identify a suitable control inhibitor compound for HTS, chymotrypsin-, trypsin-, and caspase-like activity concentration-response relationships for a panel of commercially available proteasome inhibitors were established (Figure 4 and Table S1). Out of the tested compounds, oprozomib exhibited specificity for the *T. cruzi* proteasome chymotrypsin-like active sites, which is in line with previous literature reports (9,25). Interestingly, this compounds failed to completely abolish catalytic activity in this biochemical assay. It was hypothesised that the suc-Leu-Leu-Val-Tyr-aminoluciferin substrate was not specific for the chymotrypsin-like active site of the *T. cruzi* proteasome, and residual turnover of the substrate by the trypsin- and/or caspase-like active sites resulted in incomplete apparent inhibition of chymotrypsin-like activity. To investigate this further, steady-state chymotrypsin-like activity concentration-response relationships were established for oprozomib using 20 µM and 600 µM of suc-Leu-Leu-Val-Tyr-aminoluciferin substrate. It was envisaged that in the presence of a specific chymotrypsin-like activity inhibitor, an increase in non-specific luminogenic substrate would result in an increased residual luminescence response and subsequently a reduced upper concentration-response curve plateau. The marked reduction in the upper concentration-response curve plateaus following a 30-fold increase in the suc-Leu-Leu-Val-Tyr-aminoluciferin substrate (Figure S3) and complete inhibition of *T. cruzi* proteasome chymotrypsin-like activity by the remaining tested compounds, which are also inhibitors of the trypsin- and caspase-like active sites (Figure 4 and Table S1), provided favourable evidence for the aforementioned hypothesis. These findings are in line with those reported by Kirkman *et al*, who

showed that both the β2 and β5 subunits of the *Plasmodium falciparum* proteasome were capable of hydrolysis of the fluorescence-tagged suc-Leu-Leu-Val-Tyr-AMC substrate (26). It is worth noting that bortezomib, ixazomib, and MG132 exhibited bi-phasic chymotrypsin-like activity dose-response curves. Taking the above into account, it is possible that these bi-phasic responses were a consequence of suc-Leu-Leu-Val-Tyr-aminoluciferin substrate turnover by the caspase- and/or trypsin-like active sites of the proteasome. For HTS data normalization, a control compound that can abolish *T. cruzi* proteasome catalytic activity would be preferred. With this in mind, and due to its highly potent inhibitory properties, bortezomib was selected as the control inhibitor.

Next, we compared the chymotrypsin-like pIC_{50} values of the commercial proteasome inhibitors with their pEC_{50} values obtained using a cellular *T. cruzi* epimastigote viability assay (Figure 5 and Table S1). All of the tested compounds were found to be active in the cellular assay. Epoxomicin and oprozomib exhibited equipotency between the cell-free chymotrypsin-like activity and cellular assays, while the remaining peptide-based compounds exhibited >10-fold higher potency in the cell-free versus cellular systems. Compared to a cell-free system, protein target engagement by an inhibitor in a cellular assay is dependent on a number of additional factors including cellular penetration and retention, which are heavily influenced by the physiochemical properties of the compound as well as cellular substrate concentration and affinity. Therefore, it is not unusual for greater inhibitory potency to be observed in a cell-free versus cellular assay system. The tested compounds can be clustered into peptide epoxyketone, peptide boronate, and peptide aldehyde structural classes (Figure 6), which target the catalytic active sites of the proteasome. The peptide epoxyketones are known to be irreversible proteasome inhibitors, while the boronate and aldehyde peptide analogues exhibit their effect through reversible binding mechanisms (21,25,27). The lower potency in the cellular assay for the latter two classes could thus be explained by a presumably high concentration of high affinity substrates in cells (all proteins that are marked for degradation), which is something that would affect the irreversible inhibitors less.

High-throughput screening test studies.

Following pharmacological validation of the *T. cruzi* proteasome luminescence-based assay, a number of test screening procedures were undertaken to evaluate the suitability of the assay in a high-throughput format. Firstly, the sensitivity, specificity, and robustness of the platform were tested by assaying two 384-well microplates that were randomly spiked with the control compound bortezomib at concentrations that were approximately equivalent to the IC_{30}, IC_{50}, and IC_{70} values in this biochemical assay. The assay was found to be highly sensitive, specific, and robust with a sensitivity of 100%, specificity of 99.4% (Table S2), and Z factor value of 0.87. Next, a 'Nuisance' set of 1027 compounds, selected to highlight common biochemical assay interference mechanisms (28), was tested. A good linear correlation was established between screening replicates of this compound set (R^2 = 0.95) (Figure S4). However, a high number of hits that were capable of inhibiting the biochemical response by 30% or more were identified (239 compounds; hit rate = 23.3%). Further evaluation of the interference annotations for these compounds revealed that the assay appeared to be particularly sensitive to interferers of the luciferase enzyme and other mechanisms responsible for a sustained glow-like luminescence response (Table 1).

High-throughput counter-screen (technology interference) assay development.

High levels of technology interference during early screening stages of the drug discovery process can translate into large numbers of false positive hits being selected for follow up in orthogonal assay hit-confirmation studies, which are often resource intensive and lower-throughput. In an attempt to mitigate this issue, our efforts were directed towards developing a secondary high-throughput biochemical counter-screen assay in order to de-convolute luminescence technology interferers from potential *T. cruzi* proteasome inhibitors. By exposing the luciferase reporter component of the proteasome luminescence-based assay system to varying concentrations of aminoluciferin substrate, a rapid decline in luminescence signal was observed as substrate was consumed and eventually depleted (Figure 7 a). However, it was noted that when the substrate concentration was sufficiently high (i.e. ≥2.5 μM), the rapid initial decline in signal was followed by a sustained luminescence response that lasted the duration of the experiment (i.e. 75 minutes). Bioluminescence is an adenosine triphosphate

(ATP) driven process that involves the oxidation of aminoluciferin by a luciferase enzyme resulting in the generation of a detectable photon. In order to establish a sustained glow-like luminescence response, ATP must be regenerated. Therefore, we envisaged that the luciferase reporter component of the biochemical assay comprised of an ATP reservoir, which in the presence of sufficient aminoluciferin substrate was rapidly depleted and the luminescence response became rate-limited by ATP regeneration, thereby resulting in a sustained glow-like signal. This was rationalised by the increase in the time taken to reach a sustained luminescence response when the amount of exogenous ATP in the assay system was increased (Figure 7 b). Based on these findings and calculated Z factor values, we selected an aminoluciferin substrate concentration of 5 µM (final assay concentration) and a 60 minute incubation period as desirable assay conditions.

High-throughput counter-screen (technology interference) assay validation.

In order to validate the secondary luciferase reporter counter-screen assay, screening of the 'Nuisance' compound set was performed using this assay and a total of 76 hits were identified (hit rate = 7.4%) using a 30% inhibition cut-off threshold. The counter-screen detected a large proportion of interferers of the luciferase enzyme and mechanisms responsible for a sustained glow-like luminescence response that were identified as hits using the primary *T.* cruzi proteasome chymotrypsin-like activity assay (Table 1). The inability of the counter-screen assay to detect all of the luciferase enzyme inhibitor hits could be explained by slight differences in configurations between the counter-screen and primary assays. In the case of the primary screening assay, aminoluciferin was generated *in situ* by the *T. cruzi* proteasome at presumably lower concentrations than utilised in the counter-screen assay, where an excess of the substrate was required to generate a sustained response. It was therefore likely that the counter-screen assay was less sensitive to competitive inhibitors of the luciferase enzyme compared to the primary screening assay. It is also important to appreciate that the counter-screen assay was not designed to identify non-specific sources of technology interferers such as DNA binders and redox cyclers, which were both prominent hits in the primary screening platform, and that some compounds in the 'Nuisance' set may be genuine inhibitors of the proteasome.

However, it was envisaged that removal of technology interference at the level of the luminescence based reporter system will sufficiently reduce false positive hits to allow for further down-stream hit confirmation studies using lower throughput orthogonal assay platforms.

High-throughput screening of diverse compound libraries

With the appropriate biochemical tools in place, we proceeded by screening two compound libraries comprising a total of 18,098 compounds covering traditional small-molecule chemical space using the primary *T.* cruzi proteasome chymotrypsin-like activity luminescence-based assay at a fixed compound concentration of 9.4 µM. Following this effort, we have identified 372 compounds (hit rate = 2.1%) capable of inhibiting the biochemical response by 30% or more (Figure 8). Based on our previous findings, we envisaged that the high hit rate was partially driven by technology interference at the level of the luciferase reporter system. Therefore, as an initial effort to eliminate a proportion of false positive hits prior to down-stream concentration-response assessment, the hit compounds were re-screened using the primary chymotrypsin-like activity assay as well as the secondary counter-screen assay. By application of fixed ≥30% and <45% inhibition threshold parameters for the former and latter assays, respectively, 180 hits were identified for further evaluation (Figure 9). Concentration-response assessment of these compounds using the aforementioned assays was performed, and good linear correlations were obtained between the calculated pIC_{50} values from the respective assay replicates (Figure S5 a and S5 b). From the 180 hit compounds, 163 were found to be active in the primary *T. cruzi* proteasome chymotrypsin-like activity assay (i.e. pIC_{50} >4.0) (Figure S5 a). However, from these only 39 compounds were found to be completely inactive (i.e. pIC_{50} ≤4.0) against the secondary counter screen assay (Figure S6 and Table S3), with the remaining compounds exhibiting some form of technology interference (Figure 10). Interestingly, the potency correlation between the primary chymotrypsin-like activity and counter-screen assays revealed approximately 5-fold higher pIC_{50} values for the former assay relative to the counter-screen assay. This skewed relationship could be explained by the presumably lower aminoluciferin substrate concentration present in the primary screening assay relative to the counter-screen assay, as described earlier, which would likely make the chymotrypsin-like activity assay more sensitive to potential interferers.

Conclusion.

We have successfully validated a method for the production and partial purification of *T. cruzi* proteasomes, which we have shown to exhibit the characteristic chymotrypsin-, trypsin-, and caspase-like activities. The isolated protein material was used to adapt a commercially available glow-response luminescence-based assay system into a sensitive and specific high-throughput platform aimed at identifying *T. cruzi* proteasome inhibitors. Interestingly, our findings suggested that the suc-Leu-Leu-Val-Tyr-aminoluciferin substrate used in this biochemical assay to probe proteasome chymotrypsin-like activity was not specific for the single type of *T. cruzi* proteasome active site. Instead, it appeared that a fraction of the substrate was being turned over by the trypsin- and/or caspase-like active sites of the protein. Validation of the luminescence-based biochemical assay using a 'Nuisance' compound set, designed to provide an indication of types of technology interference, revealed that the assay was prone to interference at the level of the luciferase reporter. To combat this issue, we developed a high-throughput secondary counter-screen assay that was sensitive to both luciferase inhibitors and inhibitors of the ATP-regeneration mechanism responsible for a sustained glow-like luminescence response. We then utilised the luminescence-based *T. cruzi* proteasome chymotrypsin-like activity assay to screen a total of 18,098 structurally diverse compounds. Following re-screening and technology interference de-convolution using the secondary counter-screen assay, 39 hits of interest were identified. Further evaluation of these potential *T. cruzi* proteasome inhibitors as new chemical starting points for a Chagas' disease drug discovery programme are under way.

Methods.

General.

The commercially available Proteasome-Glo™ 3-substrate system and chymotrypsin-like assay kits (Promega; catalogue no. G8531 and G8622 respectively) were assembled as per the manufacturers' protocols (29), unless stated otherwise. Briefly, Proteasome-Glo™ Buffer was used to formulate the luciferin detection reagent (containing a recombinant thermostable luciferase enzyme) to approximately 0.35% w/v at final assay concentration. The luciferin detection reagent was then mixed with Proteasome-Glo™ trypsin, caspase-, or chymotrypsin-like reagents (comprising 15 µM Z-Leu-Arg-Arg-aminoluciferin, 20 µM Z-nLeu-Pro-nLeu-Asp-aminoluciferin, or 20 µM suc-Leu-Leu-Val-Tyr-aminoluciferin substrates respectively, at final assay concentrations) and the mixture was allowed to incubate at room temperature for 60 min prior to use. *T. cruzi* proteasome buffer comprised 50 mM Tris-HCl pH 7.5; 10 mM sucrose; 5 mM $MgCl_2$; 1 mM dithiotheritol; 2 mM ATP; 150 mM NaCl, 1 mM EDTA, and 0.05 mg/mL bovine serum albumin (BSA). *T. cruzi* Silvio X10/7 strain epimastigotes were maintained *in vitro* at 28°C in RTH/foetal calf serum (FCS) culture medium (RPMI-1640 supplemented with 0.4% trypticase peptone, 0.017 M HEPES, 25 µM haemin, 10% heat inactivated FCS). Biochemical cell-free assays were performed in a 8 µL final assay volume using 384-well white low volume plates (Greiner; catalogue no. 784904) and cellular assays were performed in a 50 µL final assay volume using 384-well standard volume plates (Greiner, catalogue no. 781098). Luminescence was read using an EnVision 2102 Multilabel Reader (PerkinElmer, USA) with 0.2 s per well reading time, unless specified otherwise. DMSO or compound were added to assay plates using Echo acoustic dispensers (Labcyte, USA). Reagent addition for high-throughput screening assays was performed using an Xrd-384 liquid dispenser (FluidX, UK) and a BioFill Solo/Xrd-384 8 channel resin nozzle (0.5–200 µL) tubing cartridge (FluidX; catalogue no. 34-1003). Data analysis was performed using SigmaPlot 12.5 software, unless stated otherwise. Z factor values were calculated using the following equation:

$$Z\ factor = 1 - ((3 \times (1.483 \times (RAU\ MAD\ Max))) + (3 \times (1.483 \times (RAU\ MAD\ Min))))/(median\ RAU\ Max - median\ RAU\ Min)$$

where MAD = median absolute deviation; Max = maximum effect control samples; Min = minimum effect control samples.

T. cruzi proteasome production and partial purification.

Mid-log phase *T. cruzi* Silvio X10/7 strain cells were harvested by centrifugation (900 g, 35 min). The resulting cell pellet was resuspended in Dulbecco's phosphate buffered saline (DPBS) and the cells were counted using a Casy® Cell counter+ system. 2×10^{10} cells were pelleted in a 50 mL conical tube (900 g, 15min). Cell pellets were then inactivated by three freeze-thaw cycles and stored at –80°C. To validate biological inactivation, approximately 10% of the pellet by weight was resuspended in RTH/FCS media and incubated at 28 °C for 6 weeks. Absence of cell growth after 6 weeks was considered evidence of inactivation. For proteasome purification, *T. cruzi* pellets were thawed on ice, resuspended, and diluted in an equal volume of double strength sucrose lysis buffer (100 mM Tris-HCl pH 7.5; 500 mM sucrose; 10 mM $MgCl_2$; 2 mM dithiotheritol; 4 mM ATP; 100 mM NaCl, 2 mM EDTA), followed by further dilution using single strength sucrose lysis buffer to afford a cellular concentration of 2×10^9 cells/mL. The resulting suspension was passed through a continuous flow cell disruptor (Constant Systems Limited, UK) at 20 KPSI to lyse the cells. The lysate was then clarified by centrifugation at 20,000 g at 4°C for 30 min, and the resulting supernatant was ultra-centrifuged at 300,000 g 4°C for 120 min to form a pellet. The pellet was then resuspended using 2 mL of *T. cruzi* proteasome buffer (without BSA) per litre of original *T. cruzi* growth, and solubilized by rolling at 4 °C for 30–60 minutes. Insoluble material was removed by centrifugation at 20,000 g at 4°C for 20 min. The sample was then passed through a 0.2 µm syringe filter, and purified using a 100 mL Superose 6 gel filtration column at a flow rate of 0.5 mL/min.

Activity-based characterisation of _T. cruzi_ proteasome.

Four microliters of each undiluted 2 mL gel-filtration fraction was incubated at room temperature with either epoxomicin (Sigma Aldrich, catalogue no. E3652; 5 µM and 0.5% v/v DMSO final concentrations) or DMSO (0.5% v/v final assay concentration) at room temperature for 60 min. Next, 4 µL of the luciferin detection and Proteasome-Glo™ chymotrypsin-like reagent mixture was added to initiate the biochemical reaction. The reaction was allowed to proceed at room temperature for 20 min, after which luminescence was read. Data were acquired from a single replicate (n = 1). Gel-filtration fractions displaying chymotrypsin-like activity amenable to epoxomicin inhibition were pooled together (Figure S1). Four microliters of the pooled protein material was then added to 4 µL of luciferin detection and Proteasome-Glo™ chymotrypsin-, trypsin- or caspase-like reagent mixtures in the presence of either epoxomicin (5 µM and 0.5% v/v DMSO final assay concentrations) or DMSO (0.5% v/v final assay concentration). Luminescence was read immediately after, and then every 90 s for 75 min. Data were acquired from 6 technical replicates (n = 6).

Primary assay development and kinetic parameter determination.

Assay linearity and the optimal amount of *T. cruzi* proteasome for screening was determined by first serially diluting (1 in 2; CMF = 0.5) the proteasome stock solution in proteasome buffer to generate 10 additional concentrations. Next, 4 µL of each of the *T. cruzi* proteasome solutions was added to 4 µL of the luciferin detection and Proteasome-Glo™ chymotrypsin-like reagent mixture. Luminescence was read immediately after, and then every 90 s for 75 min. Data were acquired from 5 technical replicates (n = 5). To calculate the Michaelis constant and identify the optimal amount of chymotrypsin-like suc-Leu-Leu-Val-Tyr-aminoluciferin substrate for screening, the Proteasome-Glo™ chymotrypsin-like assay (Promega; catalogue no. G8622) luciferin detection reagent (comprising luciferase enzyme in Proteasome-Glo™ buffer) was prepared as per the manufacturers' protocol (29). A 1200 µM solution (600 µM final assay concentration) of the substrate was prepared and subsequently serially diluted (1 in 2; CMF = 0.5) using the luciferin detection reagent to generate 8 additional concentrations. Next, 4 µL of each of the luciferin detection and substrate solution mixtures were added to 4 µL of partially purified *T. cruzi* proteasome that was diluted 1 in 4 (CMF =

0.25) from the original stock using proteasome buffer. Luminescence was read immediately after, and then every 90 s for 75 min. Data were acquired from 3 technical replicates (n = 3). The Michaelis constant (K_m) was obtained by fitting all of the individual replicate data to the Michaelis-Menten equation shown below:

$$v = \frac{V_{max}[S]}{K_m + [S]}$$

DMSO tolerance.

Partially purified *T. cruzi* proteasome stock solution was diluted 1 in 4 (CMF = 0.25) using proteasome buffer, and 4 µL of the diluted solution was added to varying volumes of DMSO (corresponding to 1% v/v, 0.5% v/v, 0.25% v/v, and 0.125% v/v final assay concentrations). Next, 4 µL of the luciferin detection and Proteasome-Glo™ chymotrypsin-like reagent mixture was added to initiate the biochemical reaction. Luminescence was read immediately after, and then every 90 s for 75 min. Data were acquired from 6 technical replicates (n = 6).

Cell-free pIC_{50} determinations for commercial compounds.

Partially purified *T. cruzi* proteasome stock solution was diluted 1 in 4 (CMF = 0.25) using proteasome buffer, and 4 µL of the diluted solution was incubated at room temperature for 60 min in varying concentrations of compound (oprozomib, bortezomib, ixazomib, and MG132: Selleckchem, catalogue no. S7049, S1013, S2180, and S2619 respectively; MG115: Enzo Life Sciences, catalogue no. ALX-260-091-M005; epoxomicin: Sigma-Aldrich, catalogue no. E3652; 12 final assay concentrations ranging from 3.09×10^{-5} M to 1.11×10^{-9} M at 1 in 3 dilution increments). Next, 4 µL of luciferin detection and Proteasome-Glo™ chymotrypsin-, caspase, or trypsin-like reagent mixtures were added to initiate the biochemical reaction. The reaction was allowed to proceed at room

temperature for 60 min, after which luminescence was read. Data were acquired from 4 independent replicates (n = 4). Relative luminescence unit (RLU) data were normalized to percentage inhibition (% inhibition) values relative to 100% effect (DMSO, 1% v/v final assay concentration in the absence of *T. cruzi* proteasome enzyme) and 0% effect (DMSO, 1% v/v final assay concentration with *T. cruzi* proteasome enzyme) control populations using Microsoft Excel 2013 software. IC_{50} values were calculated by fitting the concentration-response data for each independent replicate separately to either a four- parameter logistic model or a seven-parameter logistic model with the bottom curve plateau parameter constrained to zero, as shown below.

Four-parameter logistic model:

$$y = Min + \frac{Max - Min}{1 + \left(\frac{x}{IC}\right)^{-Hillslope}}$$

Seven-parameter logistic model:

$$y = \left(Max\_1 + \left(\frac{Min - Max\_1}{1 + \left(\left(\frac{x}{IC_{50}\_1} \right)^{Hillslope\_1} \right)} \right) \right)$$

The IC_{50} parameters were then used to calculate the pIC_{50} values using the below equation, followed by a calculation of a mean pIC_{50} for each compound:

$$pIC_{50} = (-\log(IC_{50}[M]))$$

Where bi-phasic concentration-response curves were observed, pIC_{50} values for the dominant curve were reported. Figures were generated by fitting the mean concentration-response data for each compound using the aforementioned models.

Cell-free concentration-response relationships using 20 µM and 600 µM substrate.

The Proteasome-Glo™ chymotrypsin-like assay (Promega: catalogue no. G8622) luciferin detection reagent (comprising luciferase enzyme in Proteasome-Glo™ buffer) was prepared as per the manufacturers' protocol (29). A 1200 µM (600 µM final assay concentration) and 40 µM (20 µM final assay concentration) solution Proteasome-Glo™ chymotrypsin-like reagent was prepared using the luciferin detection reagent as a diluent, and the mixtures were incubated at room temperature for 60 minutes. Partially purified stock *T. cruzi* proteasome solution was diluted 1 in 4 (CMF = 0.25) using proteasome buffer, and 4 µL of the diluted solution was added to varying concentrations of oprozomib (Selleckchem, catalogue no. S7049) (12 final assay concentrations ranging from 3.09×10^{-5} M to 1.11×10^{-9} M at 1 in 3 dilution increments). Next, 4 µL of either 40 µM or 1200 µM Proteasome-Glo™ chymotrypsin-like reagent were added to initiate the biochemical reaction. The reaction was allowed to proceed at room temperature for 60 min, after which luminescence was read. Data were acquired from 3 independent replicates (n = 3), and were processed as described above for the cell-free pIC_{50} determination experiments.

Cellular pEC_{50} determinations for commercial compounds.

T. cruzi Silvio X10/7 strain epimastigotes (25 µL at 5×10^5 cells/mL) were incubated at 28°C in 5% CO_2 for 96 h in either a fixed concentration of control compound (Nifurtimox: Sigma Aldrich, catalogue no. N3415-25MG; 4.98×10^{-5} M final assay concentration) or varying concentrations of test compound (oprozomib, bortezomib, ixazomib, MG132, MG115, and epoxomicin; 10 final assay concentrations ranging from 4.98×10^{-5} M to 2.49×10^{-9} M at 1 in 3 dilution increments). For the cell viability read-out, BacTiter-Glo™ Microbial Cell Viability Reagent (Promega, catalogue no. G8230) was added to each well (25 µL) and incubated at room temperature for 5 min. Plates were then sealed with clear film and luminescence was read using a Victor 3 (PerkinElmer, USA) or PHERAstar FS (BMG LABTECH, Germany) plate reader with a 0.5 s per well reading time. Data for epoxomicin

were obtained from three independent replicates (n = 3), and data for all remaining compounds were acquired from four independent replicates (n = 4). RLU data were normalized to % inhibition values relative to 100% effect (Nifurtimox) and 0% effect (DMSO, 1% v/v final assay concentration) control populations. Normalized data for each independent replicate were fitted separately to a four-parameter logistic regression model and pEC_{50} (i.e. $-\log(EC_{50}[M])$) values were calculated using IBDS ActivityBase 8.1.2.12 software, after which a mean pEC_{50} value for each compound was calculated.

Secondary counter-screen assay development.

In order to identify the optimum amount of aminoluciferin substrate (Stratech: catalogue no. 13415-AAT) for screening, a 20 µM solution (10 µM final assay concentration) of substrate was prepared and subsequently serially diluted (1 in 2; CMF = 0.5) using the proteasome buffer to generate 10 additional concentrations. To test the dependence of the assay on exogenous ATP, 10 µM aminoluciferin substrate solutions (5 µM final assay concentration) were also prepared in proteasome buffer either lacking ATP (Buffer A) or containing 4 mM ATP (Buffer B). Next, 4 µL of each of the substrate solutions was added to 4 µL of luciferin detection reagent. Luminescence was read immediately after, and then every 90 s for 75 min. Data were acquired from 5 technical replicates for each experiment (n = 5).

High-throughput screening test studies.

To test assay sensitivity, specificity, and suitability in a high-throughput format, partially purified stock *T. cruzi* proteasome solution was diluted 1 in 8 (CMF = 0.125) using proteasome buffer and 4 µL of the diluted solution was added to two assay plates containing bortezomib (Selleckchem: catalogue no. S1013). Bortezomib was randomly distributed across a total of 22 positions per plate at final assay concentrations approximately equivalent to the IC_{70} (79 nM and DMSO 1% v/v), IC_{50} (17 nM and DMSO 1% v/v), and IC_{30} (4 nM and DMSO 1% v/v) values for the compound. With the exception of the control columns, all remaining plate wells contained DMSO only (1% v/v final assay

concentration). The plates were allowed to incubate at room temperature for 60 min, after which 4 µL of Proteasome-Glo™ chymotrypsin-like reagent was added to initiate the biochemical reaction. The reaction was allowed to proceed at room temperature for 60 min, after which luminescence was read. RLU values were normalized to % inhibition values relative to 100% effect (10 µM bortezomib and DMSO 1% v/v final assay concentrations) and 0% effect (DMSO, 1% v/v final assay concentration) control populations using the Microsoft Excel 2013 software. A hit identification threshold of 30% inhibition was set, and the percentage sensitivity and specificity were calculated using the below equations.

Sensitivity:

$$\text{Percentage sensitivity} = \frac{\text{TP}}{\text{TP} + \text{FN}} \times 100$$

where, TP = true positive; FN = false negative.

Specificity:

$$\text{Percentage specificty} = \frac{\text{TN}}{\text{FP} + \text{TN}} \times 100$$

where, TN = true negative; FP = false positive.

Single point high-throughput screening.

In the case of the primary assay, 4 µL of partially purified *T. cruzi* proteasome that was diluted 1 in 8 (CMF = 0.125) from the original stock using proteasome buffer was added to assay plates containing either technology interference 'Nuisance' compounds (1027 compounds; 10 µM and DMSO 1% v/v final assay concentrations), or structurally diverse compounds exploring drug-like chemical space from the Dundee Drug Discovery Unit library (9,257 compounds) and Global Health Chemical

Diversity Library (GHCDL) (8,841 compounds) libraries (9.4 µM and DMSO 1% v/v final assay concentration). The plates were allowed to incubate at room temperature for 60 min, after which 4 µL of luciferin detection and Proteasome-Glo™ chymotrypsin-like reagent mixture was added to initiate the biochemical reaction. The reaction was allowed to proceed at room temperature for 60 min, after which luminescence was read. For the secondary counter-screen assay, 4 µL of 10 µM aminoluciferin solution (5 µM final assay concentration) formulated in proteasome buffer was added to the compound containing assay plates, followed by 4 µL of luciferin detection reagent to initiate the biochemical reaction. The plates were allowed to incubate at room temperature for 60 min, after which luminescence was read. RLU values were normalized to % inhibition values relative to 100% effect (9.4 µM bortezomib and 1% v/v DMSO final assay concentration for the primary assay, and 1% v/v DMSO in the absence of luciferase detection reagent for the secondary counter-screening assay) and 0% effect (DMSO, 1% v/v final assay concentration) control populations. For the 'Nuisance' compound set, primary assay screening data were acquired from 2 independent replicates (n = 2), while the secondary assay counter-screen data were acquired from a single replicate (n = 1). For initial single point high-throughput screening of the two diversity compound sets, data were acquired from a single replicate (n = 1) and follow up screening data of identified hits using both the primary and secondary-counter screen assays were acquired for two independent replicates (n = 2). Compounds exhibiting ≥30% and ≥45% inhibition in the primary and secondary counter-screen assays, respectively, were identified as hits. Data were processed using IBDS ActivityBase 8.1.2.12 and Dotmatics Limited Vortex v2017.08.69598-59-s software.

Hit compound cell-free pIC_{50} determinations.

Primary screen and secondary counter-screen biochemical assays were performed as described above for the single-point high-throughput screening experiments using assay plates containing varying concentrations of compound (10 final assay concentrations ranging from 9.90×10^{-5} M to 5.52×10^{-9} M at 1 in 3 dilution increments). Data were acquired from 2 independent replicates (n = 2) for both the primary and counter-screen assays, and were subsequently processed using IBDS ActivityBase

8.1.2.12 and Dotmatics Limited Vortex v2017.08.69598-59-s software. pIC_{50} values were determined by fitting the data to a four parameter logistic model.

Ancillary Information.

Supporting Information: fraction testing of *T. cruzi* proteasome, chymotrypsin-like activity in the presence of different concentrations of DMSO, cell-free pIC_{50} and cellular pEC_{50} values for commercial inhibitors, concentration-response curves for oprozomib in the presence of low and high substrate, primary biochemical assay sensitivity and specificity calculations, high-throughput screen of 'Nuisance' set compounds, pIC_{50} correlation plots for primary and secondary counter-screen assay replicates, structures of 39 hit compounds, and primary assay pIC_{50} values for the 39 hit compounds.

Author Contributions: F. Z., L. S. T and M. D. R. conceived the research; F. Z. and M. D. R. wrote the manuscript with scientific input from L. S. T., D. W. G., S. M. S., and L. S.; F. Z. developed the primary and counter-screen biochemical assays, performed the validation and screening experiments, and analyzed the data; D. J. developed the methods for *T. cruzi* parasite growth and inactivation, and together with L. S. produced the lysates for *T. cruzi* proteasome purification; S. M. S. developed the methods for partial purification of the *T. cruzi* proteasome, and together with A. S. supplied the partially purified protein for assay development and screening; L. S. performed the cellular potency assays; P. D. C. pre-processed the raw screening data from the 'Nuisance' sets; and A. C. provided the interference annotations for the 'Nuisance' compound set hits.

Acknowledgement: The authors would like to acknowledge the Wellcome Trust for funding (Grants 204672/Z/16/Z and 203134/Z/16/Z), and the support of the Drug Discovery Unit compound management and data management teams. We would also like to acknowledge GSK for provision of

the 'Nuisance' compound set for screening against the *T. cruzi* proteasome primary and counter-screen assays. The authors have no conflicting interests.

Abbreviations Used: ATP, adenosine triphosphate; BSA, bovine serum albumin; CMF, concentration multiplication factor; DMSO, dimethyl sulfoxide; DPBS, Dulbecco's phosphate buffered saline; FN, false negative; FP, false positive; FTS, foetal calf serum; GSK, GlaxoSmithKline; HTS, high-throughput screening; MAD, median absolute deviation; RLU, relative luminescence units; *T. cruzi, Trypanosoma cruzi*; TN, true negative; TP; true positive.

References

1. Conners, E. E., Vinetz, J. M., Weeks, J. R., and Brouwer, K. C. (2016) A global systematic review of Chagas disease prevalence among migrants. *Acta trop.* 156, 68–78. DOI:10.1016/j.actatropica.2016.01.002 (2016).

2. Perez-Molina, J. A., and Molina, I. Chagas disease. (2018) *Lancet*. 391, 82–94. DOI:10.1016/S0140-6736(17)31612-4.

3. Sabino, E. C., Ribeiro, A. L., Salemi, V. M., Di, L. O. C., Antunes, A. P., Menezes, M. M., Ianni, B. M., Nastari, L., Fernandes, F., Patavino, G. M., Sachdev, V., Capuani, L., de Almeida-Neto, C., Carrick, D. M., Wright, D., Kavounis, K., Goncalez, T. T., Carneiro-Proietti, A. B., Custer, B., Busch, M. P., and Murphy, E. L. (2013) Ten-year incidence of Chagas cardiomyopathy among asymptomatic Trypanosoma cruzi-seropositive former blood donors. *Circulation*. 127, 1105–1115. DOI:10.1161/CIRCULATIONAHA.112.123612.

4. Sperandio da Silva, G. M., Mediano, M. F. F., Hasslocher-Moreno, A. M., Holanda, M. T., Silvestre de Sousa, A., Sangenis, L. H. C., Brasil, P. E. A. A. D., Mejja, R. A., Fux, C. P., Cubides, J. C., Saraiva, R. M., and Brum-Soares, L. M. (2017) Benznidazole treatment safety: the Medecins Sans

562 Frontieres experience in a large cohort of Bolivian patients with Chagas' disease. *J. Antimicrob.*
563 *Chemother.* 72, 2596–2601. DOI:10.1093/jac/dkx180.

564 5. Torrico, F., Gascon, J., Ortiz, L., Alonso-Vega, C., Pinazo, M., Schijman, A., Almeida, I. C., Alves,
565 F., Strub-Wourgraft, N., and Ribeiro, I. (2018) Treatment of adult chronic indeterminate Chagas
566 disease with benznidazole and three E1224 dosing regimens: a proof-of-concept, randomised,
567 placebo-controlled trial. *Lancet Inf. Dis.* 18, 419–430, DOI:10.1016/S1473-3099(17)30538-8 (2018).

568 6. Molina, I., Prat, J. G., Salvador, F., Trevino, B., Sulleiro, E., Serre, N., Pou, D., Roure, S., Cabezos,
569 J., Valerio, L., Blanco-Grau, A., Sánchez-Montalvá, A. (2014) Randomized trial of posaconazole and
570 benznidazole for chronic Chagas' disease. *N. Engl. J. Med.* 370, 1899–1908,
571 DOI:10.1056/NEJMoa1313122.

572 7. Pena, I, Manzano, M.P., Cantizani. J., Kessler, A., Alonso-Padilla, J., Bardera, A. I., Alvarez, E.,
573 Colmenarejo, G., Cotillo, I., Roquero, I., de Dios-Anton, F., Barroso, V., Rodriguez, A., Gray, D. W.,
574 Navarro, M., Kumar, V., Sherstnev, A., Drewry, D. H., Brown, J. R., Fiandor, J. M., and Martin, J. J.
575 (2015) New compound sets identified from high throughput phenotypic screening against three
576 kinetoplastid parasites: an open resource. *Sci. Rep.* 5, 8771. DOI:10.1038/srep08771.

577 8. Bethesda (MD): National Center for Biotechnology Information (US). (2010) *Probe Reports from*
578 *the NIH Molecular Libraries Program.* https://www.ncbi.nlm.nih.gov/books/NBK47352/ (accessed
579 Aug 27, 2018).

580 9. Khare, S., Nagle, A.S., Biggart, A., Lai, Y. H., Liang, F., Davies, L. C., Barnes, S. W., Mathison,
581 C. J. N., Myburgh, E., Gay, M., Gillespie, J. R., Liu, X., Tan, J. L., Stitson, M., Rivera, I. C., Ballard,
582 J., Yeh, V., Groessl, T., Federe, G., Kohn, H. X. Y., Venable, J. D., Bursulaya, B., Shapiro, M.,
583 Mishra P. K., Spraggon, G., Brock, A., Mottram, J. C., Buckner, F. S., Rao, S. P. S., Wen, B. G.,
584 Walker, J. R., Tuntland, T., Moleteni, V., Glynne, R. J., and Supel, F. (2016) Proteasome inhibition
585 for treatment of leishmaniasis, Chagas disease and sleeping sickness. *Nature*. 537, 229–233,
586 DOI:10.1038/nature19339.

587 10. Keenan, M., Alexander, P. W., Chaplin, J. H., Abbott, M. J., Diao, H., Wang, Z., Best, W. M.,
588 Perez, C. J., Cornwall, S. M., Keatley, S. K., Thompson, R. C., Charman, S. A., White, K. L., Ryan,
589 E., Chen, G., Ioset, J. R., von Geldern, T. W., and Chatelain, E. (2013) Selection and optimization of
590 hits from a high-throughput phenotypic screen against Trypanosoma cruzi. *Future Med. Chem.* 5,
591 1733–1752. DOI:10.4155/fmc.13.139.

592 11. Alonso-Padilla, J., and Rodriguez, A. (2014) High throughput screening for anti-Trypanosoma
593 cruzi drug discovery. *PLoS Negl. Trop. Dis.* 8, e3259. DOI:10.1371/journal.pntd.0003259.

594 12. Chatelain, E., and Ioset, J. R. (2018) Phenotypic screening approaches for Chagas disease drug
595 discovery. *Expert Opin. Drug Discov.* 13, 141–153. DOI:10.1080/17460441.2018.1417380.

596 13. Wyllie, S., Brand, S., Thomas, M., De Rycker, M., Chung, C., Pena, I., Bingham, R. P., Bueren-
597 Calabuig, J. A., Cantizani, J., Cebrian, D., Craggs, P. D., Ferguson, L., Goswami, P., Hobrath, J.,
598 Howe, J., Jeacock, L., Ko, E., Korczynska, J., MacLean, L., Manthri, S., Martinez, M. S., Mata-
599 Cantero, L., Moniz, S., Nühs, A., Osuna-Cabello, M., Pinto, E., Riley, J., Robinson, S., Rowland, P.,
600 Simeons, F. R. C., Shishikura, Y., Spinks, D., Stojanovski, L., Thomas, J., Thompson, S., Gaza, E. V.,
601 Wall, R. J., Zuccotto, F., Horn, D., Ferguson, M. A. J., Fairlamb, A. H., Fiandor, J. M., Martin, J.,
602 Gray, D. W., Miles, T. J., Gilbert, I. H., Read, K. D., Marco, M., and Wyatt, P. G. (2019) Preclinical
603 candidate for the treatment of visceral leishmaniasis that act through proteasome inhibition. *Proc.*
604 *Natl. Acad. Sci. U. S. A.* 116, 9318–9323. DOI: 10.1073/pnas.1820175116.

605 14. Ciechanover, A. (2017) Intracellular protein degradation: from a vague idea thru the lysosome and
606 the ubiquitin-proteasome system and onto human diseases and drug targeting. *Best Pract. Res., Clin.*
607 *Haematol.* 30, 341–355. DOI:10.1016/j.beha.2017.09.001.

608 15. Cromm, P. M., Crews, C. M. (2017) The proteasome in modern drug discovery: second life of a
609 highly valuable drug target. *ACS Cent. Sci.* 3, 830–838. DOI:10.1021/acscentsci.7b00252.

610 16. Kisselev, A. F., and Goldberg, A. L. (2015) Monitoring activity and inhibition of 26S proteasomes
611 with flurogenic peptide substrates. *Methods Enzymol*. 398, 364–378. DOI:10.1016/S0076-
612 6879(05)98030-0.

613 17. Tanaka, K. (2009) The proteasome: overview of structure and functions. *Proc. Jpn. Acad. Ser. B.*
614 *Phys. Biol. Sci.* 85, 12–36. DOI:10.2183/pjab.85.12.

615 18. Ng, C. L., Fidock, D. A., and Bogyo, M. (2017) Protein degradation systems as antimalarial
616 therapeutic targets. *Trends Parasitol.* 33, 731–743. DOI:10.1016/j.pt.2017.05.009.

617 19. Waring, M. J., Arrowsmith, J., Leach, A. R., Leeson, P. D., Mandrell. S., Owen, R. M.,
618 Pairaudeau, G., Pennie, W. D., Pickett, S. D., Wang, J., Wallace, O., Weir, A. (2015) An analysis of
619 the attrition of drug candidates from four major pharmaceutical companies. *Nat. Rev. Drug Discov.*
620 14, 475–486. DOI:10.1038/nrd4609.

621 20. O'Brien, M. A., Moravec, R. A., Riss, T. L., and Bulleit, R. F. (2015) Homogenous,
622 bioluminescent proteasome assays. *Methods Mol. Biol.* 1219, 95–114. DOI:10.1007/978-1-4939-
623 1661-0_9.

624 21. Kisselev, A. F., and Goldberg, A. L. (2001) Proteasome inhibitors: from research tools to drug
625 candidates. *Chem. Biol.* 8, 739–758. DOI:10.1016/S1074-5521(01)00056-4.

626 22. Meng, L., Mohan, R., Kwok, B. H., Eloffson, M., Sin, N., and Crews, C. M. (1999) Epoxomicin, a
627 potent and selective proteasome inhibitor, exhibits in vivo antiinflammatory activity. *Proc Natl. Acad.*
628 *Sci. U. S. A.* 96, 10403–10408. DOI:10.1073/pnas.96.18.10403.

629 23. Stein, R. L., Melandri, F., and Dick, L. (1996) Kinetic characterization of the chymotryptic
630 activity of the 20S proteasome. *Biochemistry.* 35, 3899–3908. DOI:10.1021/bi952262x.

631 24. Zhang, J., Chung, T. D. Y., and Oldenburg, K. R. (1999) A simple statistical parameter for use in
632 evaluation and validation of high throughput screening assays. *J. Biomol. Screen*. 4, 67–73. DOI:
633 10.1177/108705719900400206.

634 25. Zhou, H., Aujay, M., Bennett, M. K., Dajee, M., Demo, S. D., Fang, Y., Ho, M. N., Jing, J., Kirk,
635 C. J., Laidig, G. J., Lewis,E. R., Lou, Y., Muchamuel T., Parlati, F., Ring, E., Shenk, K. D., Shields,
636 J., Shwonek, P. J., Stanton, T., Sun, C. M., Sylvain, C., Woo, T. M., and Yang. J. (2009) Design and
637 synthesis of an orally bioavailable and selective peptide epoxyketone proteasome inhibitor (PR-047).
638 *J. Med. Chem.* 52, 3028–3038. DOI:10.1021/jm801329v.

639 26. Kirkman, L. A., Zhan, E., Visone, J., Dziedziech, A., Singh, P. K., Fan, H., Tong, X., Bruzual, I.,
640 Hara, R., Kawasaki, M., Imaeda, T., Okamoto, R., Sato, K., Michino, M., Alvaro, E. F., Guiang, L. F.,
641 Saz, L., Mota, D. J., Govindasamy, K., Wang, R., Ling, Y., Tumwebaze, P. K., Sukenick, G., Shi, L.,
642 Vendome, J., Bhanot, P., Rosenthai, P. J., Aso, K., Foley, M. A., Cooper, R. A., Kafsack, B.,
643 Doggetti, J. S., Nathan, C. F., and Lin, G. (2018) Antimalarial proteasome inhibitor reveals collateal
644 sensitivity from intersubunit interactions and fitness cost of resistance. *Proc. Natl. Ascad. Sci. USA.*
645 115, E6863–E6870. DOI:10.1073/pnas.1806109115.
646 27. Kupperman, E., Lee, E. C., Cao, Y., Bannerman, B., Fitzgerald, M., Berger, A., Yu, J., Yang, Y.,
647 Bruzzese, F., Liu, J., Blank, J., Garcia, K., Tsu, C., Dick, L., Fleming, P., Yu, L., Manfredi, M., Rolfe,
648 M., and Bolen, J. (2010) Evaluation of the proteasome inhibitor MLN9708 in preclinical models of
649 human cancer. *Cancer Res.* 70, 1970–1980. DOI:10.1158/0008-5472.CAN-09-2766.
650 28. Chakravory, S. J., Chan, J., Greenwood, M. N., Papa-Burke, I., Remlinger, K. S., Pickett, S. D.,
651 Green, D. V. S., Fillmore, M. C., Dean, T. W., Luengo, J. I., and Macarrón, R. (2018) Nuisance
652 compounds, PAINS filters, and dark chemical matter in the GSK HTS collection. *SALS Discov*.
653 23:532–545. DOI:10.1177/2472555218768497.
654 29. Promega. (2016) *Technical Bulletin. Proteasome-Glo™ Assay Systems. Instructions for use of*
655 *products G8531, G8532, G8621, G8622, G8632, G8641 and G8642.*
656 https://www.promega.co.uk/products/small-molecule-drug-discovery/drug-discovery-
657 workflow/primary-screening/proteasome_glo-assays/?catNum=G8532 (accessed Aug 27, 2018).
658

659 **Figures**

660

661 Figure 1. Chymotrypsin (a), trypsin (b), and caspase-like (c) activities of the *T. cruzi* proteasome in
662 the presence (black circles) and absence (red circles) of 5 μM epoxomicin. RLU = relative
663 luminescence units. Data shown for 6 technical replicates (n = 6); error bars represent ± SD.

664

Figure 2. Chymotrypsin-like activity plotted as a function of either *T. cruzi* proteasome concentration after a 60 min biochemical reaction (a) or time at different proteasome stock solution dilutions (b). RLU = relative luminescence units; CMF = concentration multiplication factor. Data shown for 5 technical replicates (n = 5); error bars represent ± SD. Linear regression $R^2 = 0.999$.

Figure 3. *T. cruzi* proteasome chymotrypsin-like activity plotted as a function of time in the presence of varying concentrations of suc-Leu-Leu-Val-Tyr-aminoluciferin substrate (a) or as a function of suc-Leu-Leu-Val-Tyr-aminoluciferin substrate concentration after a 60 min biochemical reaction fitted to the Michaelis-Menten model (apparent K_m = 93.5 µM (95% CI = 78.8–108.4 µM)) (b). Data shown for 3 technical replicates (n = 3); error bars represent ± SD.

Figure 4. Cell-free *T. cruzi* proteasome chymotrypsin- (black circles), trypsin- (red circles), and caspase-like (green triangles) activity concentration-response curves for a panel of commercially available proteasome inhibitors (i.e. epoxomicin, oprozomib, bortezomib, ixazomib, MG132, and MG115). Data shown for 4 independent replicates (n = 4). Error bars represent ± SD.

Figure 5. Correlation of *T. cruzi* proteasome pIC_{50} values obtained using cell-free and cellular assays for (in order from left to right) MG115, oprozomib, epoxomicin, MG132, ixazomib, and bortezomib. Circles = reversible peptide-based inhibitors. Triangles = irreversible peptide-based inhibitors. Data shown for 3–4 independent replicates (n = 3–4). Error bars represent ± SD.

Figure 6. Structures of commercially available proteasome inhibitors.

Table 1. Biochemical assay interference mechanisms identified during the screen of the 'Nuisance' compound set using the primary *T. cruzi* proteasome chymotrypsin-like activity luminescence-based assay and the secondary luciferase reporter counter-screen assay.

		Primary screen	Secondary counter-screen	
Interference mechanism	**Total[a]**	**Hits[b]**	**Hits[b]**	**Detected[c], %**
Inhibition of luminescence coupling system	39	37	33	89
PDELight™ inhibition	25	20	15	75
Luciferase inhibition	29	17	11	65
DNA binders	65	34	1	3
Redox cyclers	212	30	4	13
Zn chelators	28	5	1	20
Europium donor quenchers	26	2	0	0
Other	1014	208	23	11

[a]The total number of compounds in the 'Nuisance' set annotated with the listed interference mechanism (some compounds contain primary and secondary annotations); [b]number of hits identified from 'Nuisance' set screens containing primary and/or secondary annotations for the listed

interference mechanisms; [c]percentage of hits detected by the secondary counter-screen assay relative to the primary screen assay.

Figure 7. Luminescence response plotted as a function of time in the presence of varying concentrations of aminoluciferin substrate (a) or in the presence (red circles) or absence (black circles) of 4 mM exogenous ATP (b). Data shown for 4 technical replicates (n = 4). Error bars represent ± SD.

Figure 8. Single point high-throughput screen of 18,098 structurally diverse compounds at a concentration of 9.4 µM using the primary *T. cruzi* proteasome chymotrypsin-like activity assay. Red circles represent 372 hits exhibiting ≥30% inhibition. Mean Z factor = 0.91 ± 0.03 (SD; n = 58).

Figure 9. Single point high-throughput re-screen of 372 initial hit compounds at a concentration of 9.4 µM using the primary *T. cruzi* proteasome chymotrypsin-like activity assay and the secondary technology interference counter-screen assay. Data represent a mean of two independent replicates per assay (n = 2). Red circles represent 180 compounds that exhibit ≥30% and <45% inhibition in the primary and secondary counter-screen assays respectively. Primary assay mean Z factor = 0.88 ± 0.04 (SD; n = 4); counter-screen assay mean Z factor = 0.79 ± 0.11 (SD; n = 4).

Figure 10. A plot of the mean pIC_{50} values (n = 2) of 180 hit compounds obtained using the primary *T. cruzi* proteasome chymotrypsin-like activity assay and the secondary counter-screen assay. Red circles represent 39 compounds that were active against the former assay (pIC_{50} ≥4) and inactive against the counter-screen assay (pIC_{50} <4). Primary assay mean Z factor = 0.67 ± 0.05 (SD; n = 12); counter-screen assay mean Z factor = 0.77 ± 0.04 (SD; n = 12).

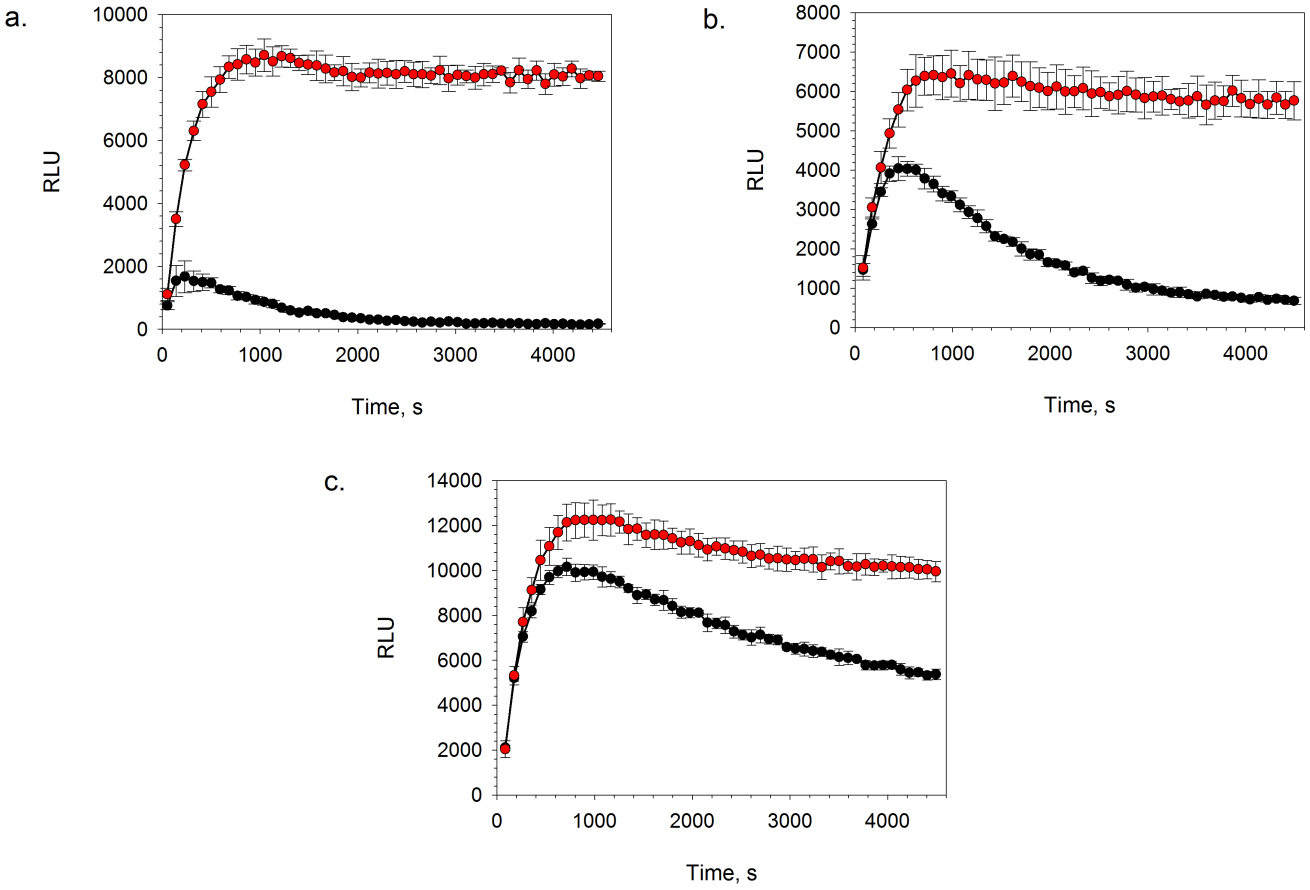

a.

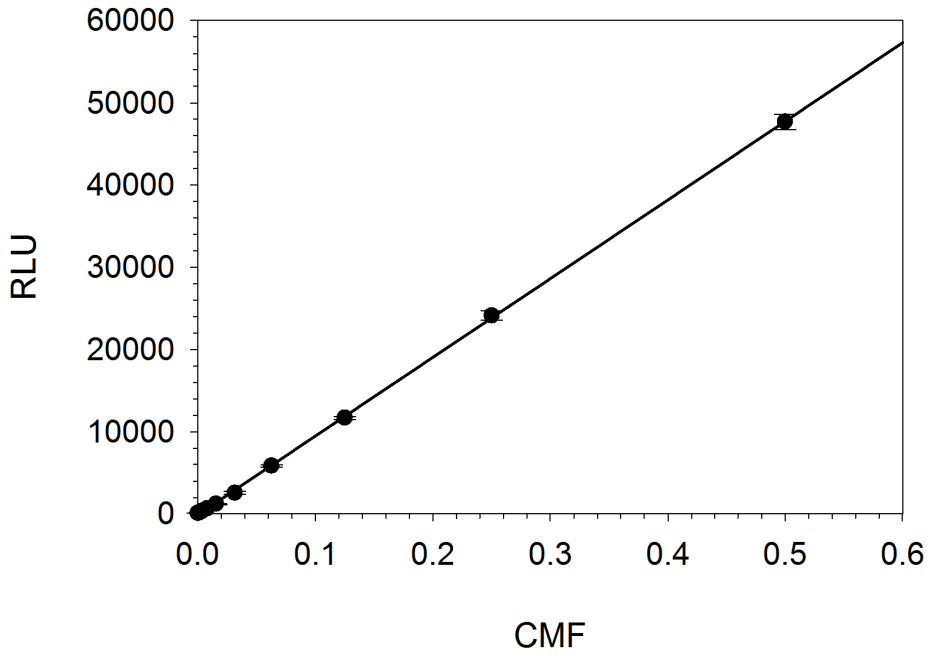

b.

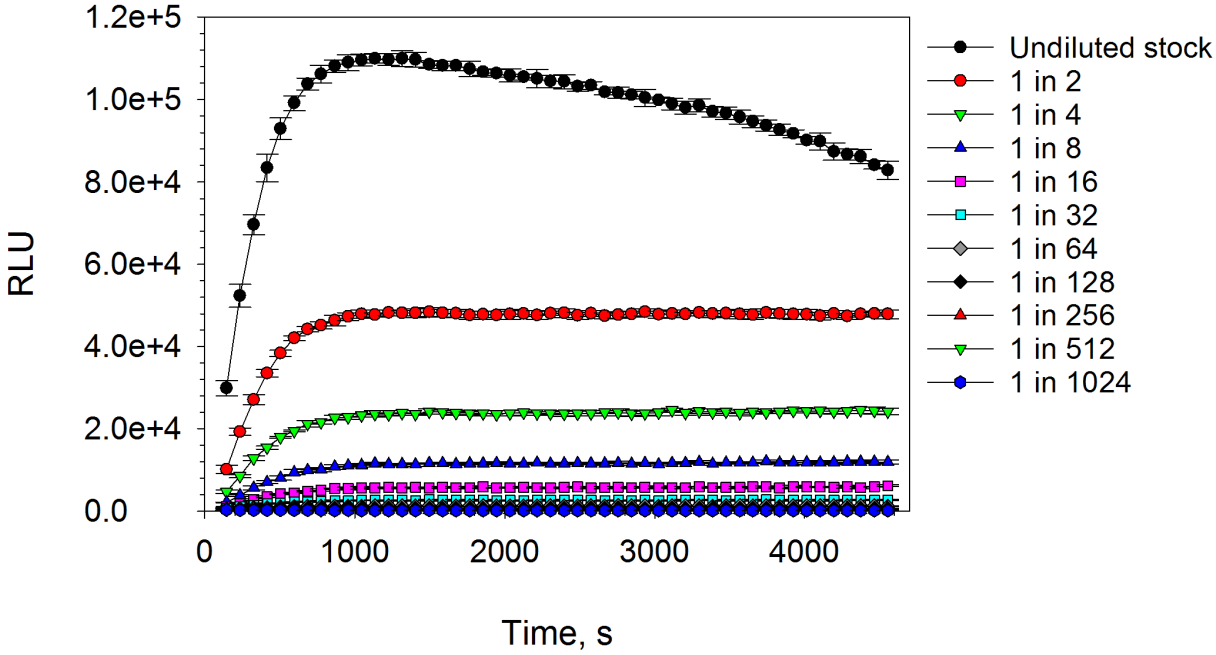

a.

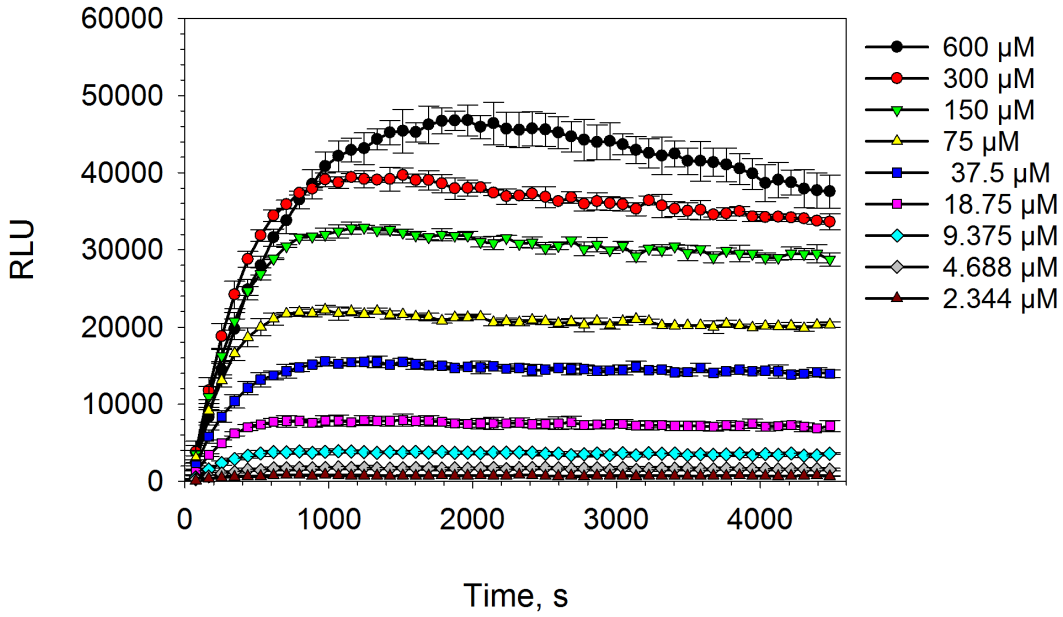

b.

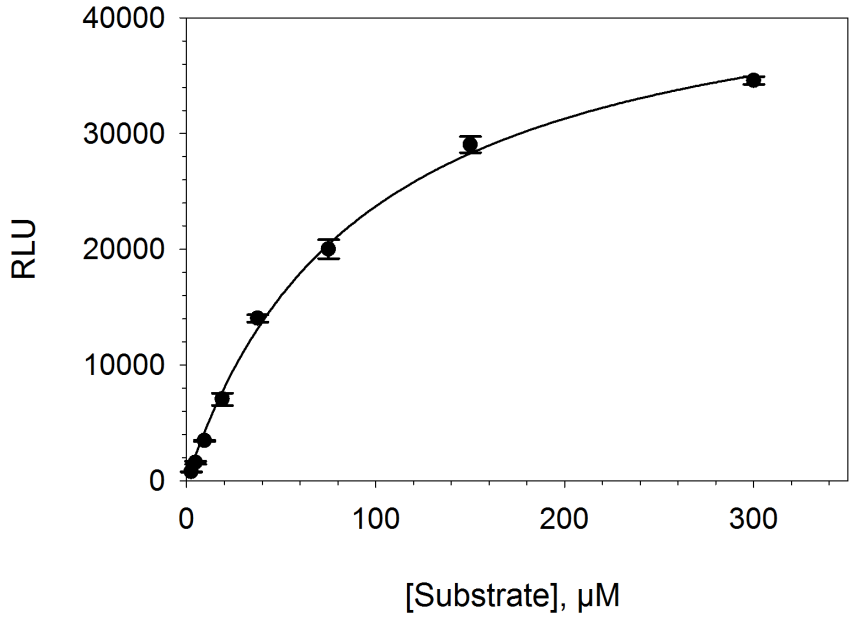

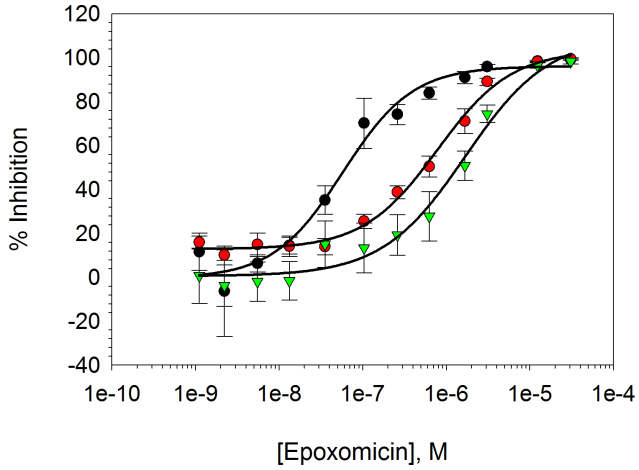

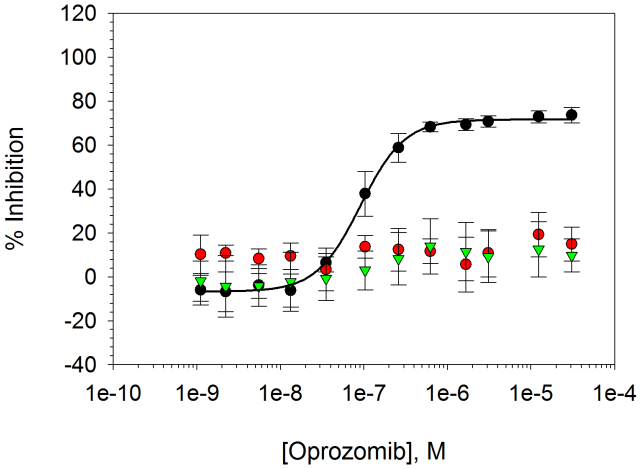

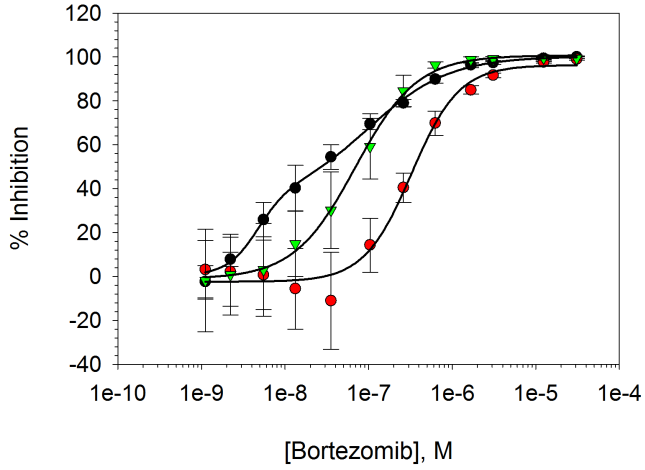

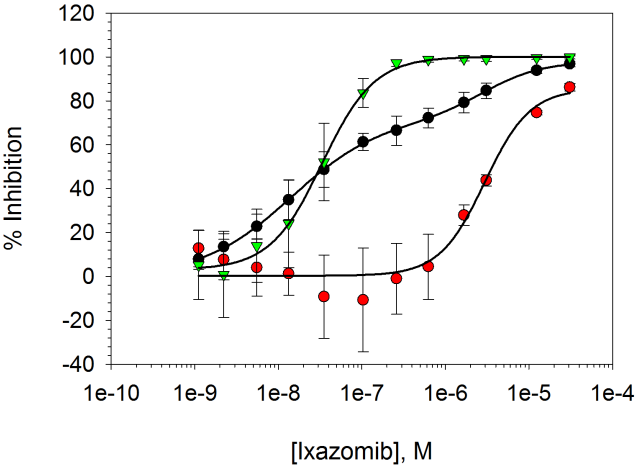

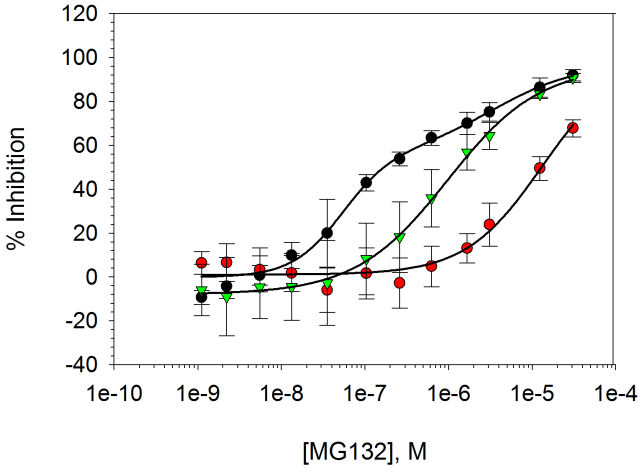

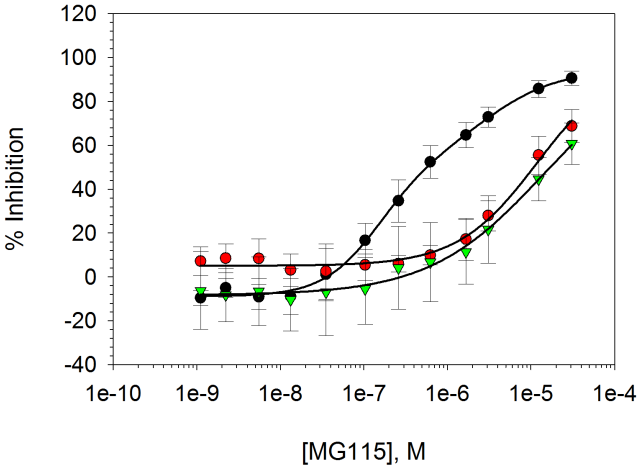

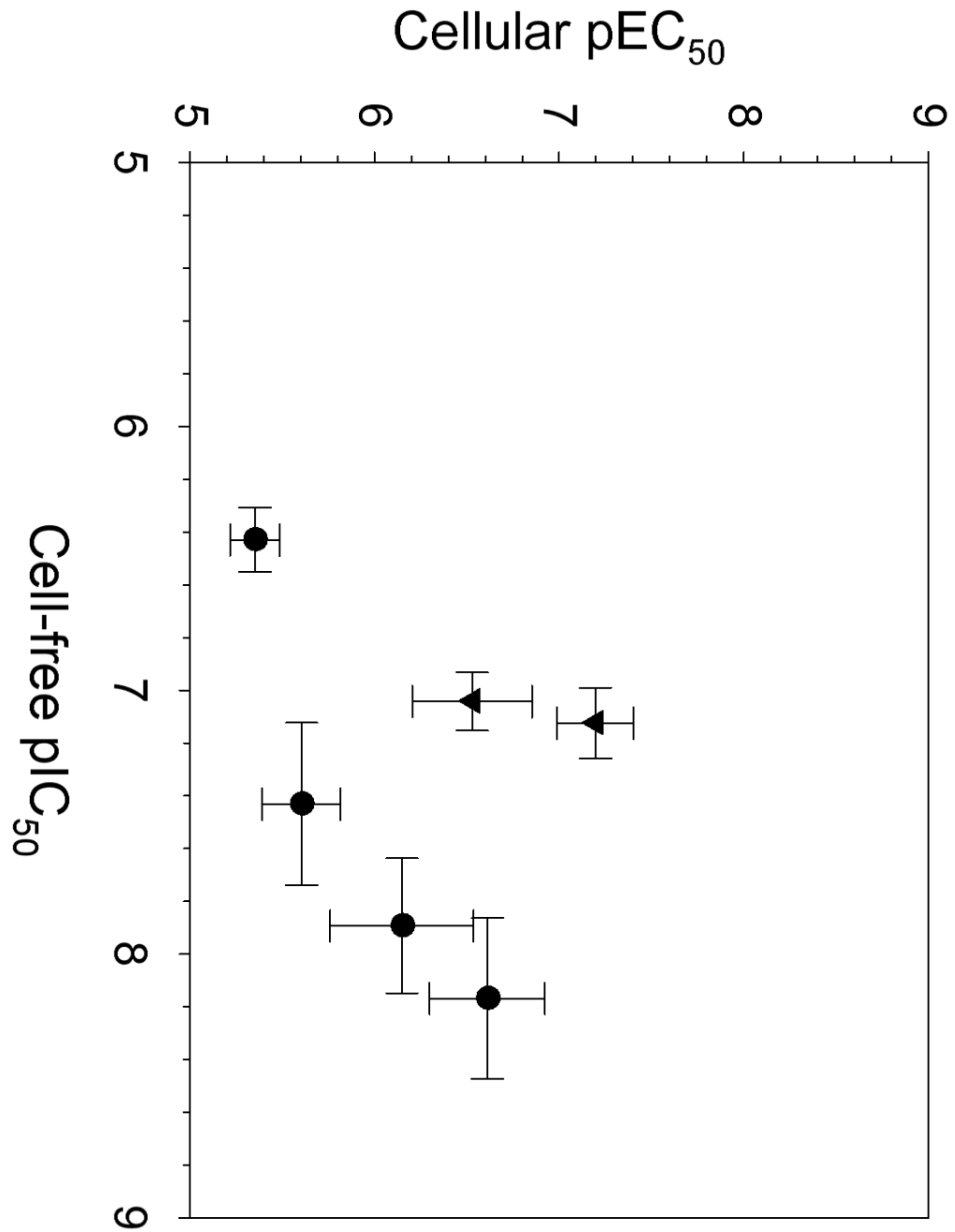

Peptide epoxyketones

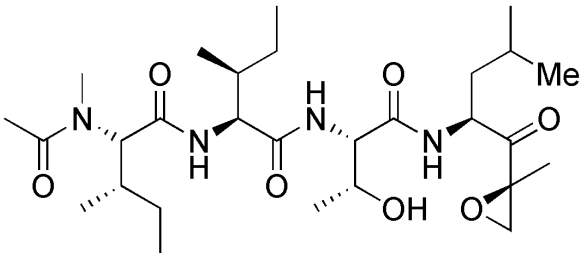

Epoxomicin

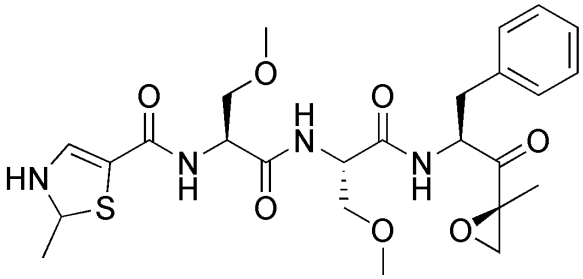

Oprozomib

Peptide boronates

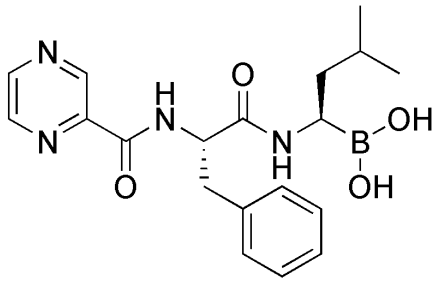

Bortezomib

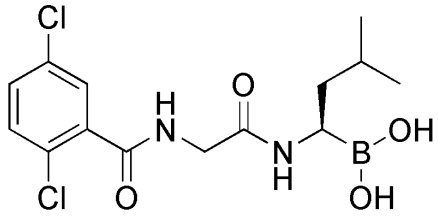

Ixazomib

Peptide aldehydes

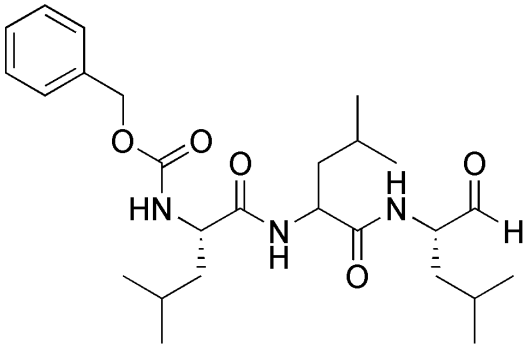

MG132

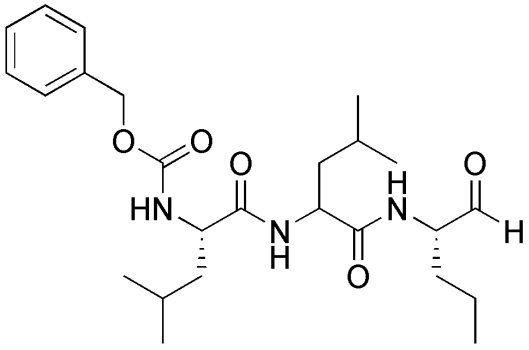

MG115

a.

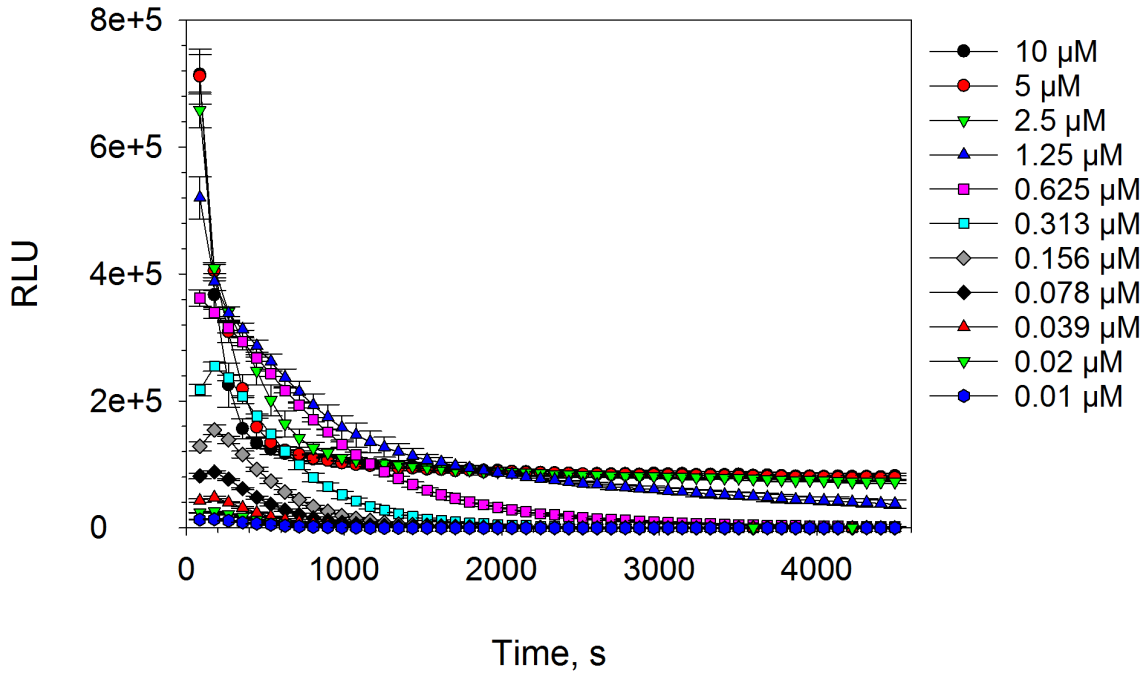

b.